

Effective Phantom Divide Crossing with Standard and Negative Quintessence

Adrià Gómez-Valent* and Alex González-Fuentes†

*Departament de Física Quàntica i Astrofísica, and Institut de Ciències del Cosmos,
Universitat de Barcelona, Av. Diagonal 647, E-08028 Barcelona, Catalonia, Spain*

Cosmic microwave background data from the *Planck* satellite, combined with baryon acoustic oscillation measurements from the Dark Energy Spectroscopic Instrument and Type Ia supernovae from various samples, provide hints of dynamical dark energy (DE). These results indicate a peak in the DE density around $z \sim 0.4 - 0.5$, with the highest significance observed when using the supernovae from the Dark Energy Survey. In this *Letter*, we show that this peak does not necessarily imply a true crossing of the phantom divide if the measured effective DE is not a single component, but a combination of standard and negative quintessence. The latter is characterized by negative energy density and positive pressure, both decreasing in absolute value and tending to 0 in the future. For appropriate values of the parameters, negative quintessence is relevant at intermediate redshifts and becomes subdominant in front of standard quintessence around $z \sim 0.4 - 0.5$, giving rise to the aforementioned peak in the DE density. We find that our model is preferred over Λ CDM at a 3.27σ CL, which is comparable to the level of exclusion found with the Chevallier-Polarski-Linder parametrization. Our analysis leaves open the possibility of negative quintessence and other exotic fields existing in the low-energy universe, potentially playing a significant role in cosmic dynamics.

Introduction – Several studies over the past decade have reported indications of dynamical dark energy (DE) [1–9], and recent observations from Type Ia supernovae (SNIa), baryon acoustic oscillations (BAO), and the cosmic microwave background (CMB) suggest a non-trivial evolution of the effective DE density, with a transition occurring around $z_{\text{cross}} \sim 0.4 - 0.5$ [10–13]. This transition implies a shift in the DE behavior – from phantom-like at earlier times ($z > z_{\text{cross}}$) to quintessence-like at lower redshifts ($z < z_{\text{cross}}$). Evidence for this crossing of the phantom divide is statistically significant, with confidence levels ranging from 96.21% to 99.97%, depending on the SNIa dataset used [12]; see also [14–16].

Constructing theoretical models that reproduce this behavior is an important challenge. It is well known that a single minimally coupled scalar field cannot account for such a crossing, see, e.g., [17–19]. Other scenarios, like those involving non-minimally coupled scalar fields [20–23], interactions in the dark sector [24, 25], $F(R)$ gravity [26, 27] or deviations from the cosmological principle [28] might be viable possibilities. In this paper, we propose an alternative framework with two scalar fields minimally coupled to gravity and demonstrate that our model is perfectly capable of explaining the latest CMB, BAO and SNIa observations.

The model – We consider the following action,

$$S \supset - \int d^4x \sqrt{-g} \sum_{I=1,2} \left[\frac{\alpha_I}{2} \partial_\mu \phi_I \partial^\mu \phi_I + \epsilon_I V_I(\phi_I) \right], \quad (1)$$

with $V_I(\phi_I) \geq 0$ the absolute value of the scalar field potentials, and α_I and ϵ_I constants equal to $+1$ or -1 , depending on the specific model we want to focus on. We

consider $\partial^2 V_I / \partial \phi_I^2 > 0$. The subscript I labels the two scalar fields. Notice that we employ natural units and only use Einstein’s summation convention for the Greek indices. The total action S also includes the Einstein-Hilbert term, the standard model of particle physics and some potential extensions of it accounting for the neutrino masses and the dark matter sector.

The modified Klein-Gordon (KG) equation that rules the scalar field dynamics in a Friedmann-Lemaître-Robertson-Walker universe takes the form,

$$\ddot{\phi}_I + 3H\dot{\phi}_I + \frac{\epsilon_I}{\alpha_I} \frac{\partial V_I}{\partial \phi_I} = 0, \quad (2)$$

where the dots denote derivatives with respect to cosmic time. The energy density and pressure of the individual scalar fields read, respectively,

$$\rho_I = \alpha_I \frac{\dot{\phi}_I^2}{2} + \epsilon_I V_I(\phi_I) \quad ; \quad p_I = \alpha_I \frac{\dot{\phi}_I^2}{2} - \epsilon_I V_I(\phi_I). \quad (3)$$

The time derivative of the energy densities is given by $\dot{\rho}_I = -3H\alpha_I\dot{\phi}_I^2$, indicating that the sign of the parameter α_I controls whether ρ_I grows or gets diluted throughout the expansion, since $H\dot{\phi}_I^2 \geq 0$. Standard quintessence (SQ) models are obtained setting $\alpha_I = \epsilon_I = +1$; phantom DE, in contrast, is realized if $\alpha_I = -1$, keeping $\epsilon_I = +1$ [29]. The combination of SQ and phantom DE that is considered in the context of the so-called quintom A models [18, 19, 30], *cannot* give rise to the behavior of the effective DE inferred from the combination of CMB+BAO+SNIa data. They can explain a transition from quintessence to phantom, but not the reverse. Quintom B models, instead, do allow for such phenomenology.

One possible realization of quintom B models is to consider SQ in conjunction with negative quintessence (NQ), as proposed in [12]. NQ is characterized by a negative

* agomezvalent@icc.ub.edu

† agonzalezfuentes@icc.ub.edu

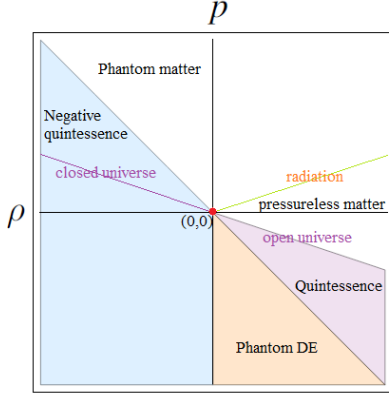


FIG. 1. EoS diagram. The pink and orange regions correspond to the SQ ($-1 \leq w \leq -1/3$) and phantom ($w \leq -1$) DE regimes, respectively. In the white region the strong energy condition is fulfilled, i.e., $\rho + 3p \geq 0$ and $\rho + p \geq 0$. In particular, non-relativistic matter ($w = 0$) and radiation ($w = 1/3$) lie within this region, satisfying $p, \rho \geq 0$. Phantom matter ($w \leq -1$) as well, with $\rho < 0$ and $p > 0$ [37–40]. The blue region is the one for species with negative energy density and decreasing absolute value. Within that region, the triangular area bounded by the “closed universe” line and the edge of the “phantom matter” region represents the domain of the NQ scenario.

energy density and a positive pressure, both with decreasing absolute values. In the context of the action (1), NQ can be implemented by setting $\alpha_I = \epsilon_I = -1$, i.e., by considering a scalar field with negative kinetic term and negative potential. Lagrangians of this sort were previously studied in [31]. The form of the scalar field equation remains as in SQ, since α_I and ϵ_I have the same sign. However, the field can gain energy during cosmic expansion, even though that energy remains negative. NQ might be affected by similar issues to those found in phantom DE due to the presence of instabilities because of rapid vacuum decay into ghosts and gravitons. This is a contrived discussion in the absence of a complete theory of quantum gravity. We will treat the model as an effective theory with the hope that either higher order derivative terms in the action or the existence of an energy cutoff for Lorentz invariance render the theory stable at the quantum level, see [31–36] for dedicated discussions. In any case, our analysis is purely classical. In the equation-of-state (EoS) diagram of Fig. 1, NQ lies in the region between the closed universe ($w = -1/3$) and phantom ($w = -1$) lines, with negative energy density and positive pressure. Phantom matter also has $\rho < 0$ and $p > 0$, but their absolute values grow with the expansion, instead of decreasing, since $w < -1$ [37–40]. This form of matter can be mimicked by a minimally coupled scalar field if $\alpha_I = +1$, $\epsilon_I = -1$.

We implement the model considering the following absolute values of the quadratic potentials for the SQ

($I = 1$) and NQ ($I = 2$) fields,

$$V_1(\phi_1) = V_0 + \frac{m_1^2}{2}\phi_1^2 \quad ; \quad V_2(\phi_2) = \frac{m_2^2}{2}\phi_2^2, \quad (4)$$

with $V_0 > 0$ playing the role of a cosmological constant and m_1 and m_2 the masses of the fields, which are real. They control the curvature of the potential and, hence, the moment in cosmic history at which the fields become dynamical. We call our model SQ+NQ, for short.

At the perturbative level, neither SQ nor NQ exhibit tachyonic nor gradient instabilities. This is easy to understand by looking at the equation for the scalar field perturbation $\delta\phi_I$, which in the synchronous gauge reads,

$$\delta\ddot{\phi}_I + 3H\delta\dot{\phi}_I + (c_s^2 k^2 + m_I^2)\delta\phi_I + \frac{\dot{h}\dot{\phi}_I}{2} = 0, \quad (5)$$

with h the trace of the metric perturbation. There is no exponential growth of $\delta\phi_I$ at any scale, since both $m_I^2 > 0$ and $c_s^2 = 1 > 0$. These instabilities are not dramatic in general if they develop in a timescale $\gtrsim \mathcal{O}(H^{-1})$, but in our model they are simply non-existent.

At sufficiently large redshifts, the SQ and NQ potentials play no important role because cosmic friction dominates over the potential term in the KG equation (2), so $\dot{\phi}_I \sim 0$. At those epochs, ϕ_1 and ϕ_2 are frozen and these two components essentially behave jointly as a cosmological constant with value

$$V_{\text{ini}} = V_0 + \frac{1}{2}(m_1^2\phi_{1,\text{ini}}^2 - m_2^2\phi_{2,\text{ini}}^2). \quad (6)$$

The scalar field ϕ_I starts to roll down the potential $V_I(\phi_I)$ when $H \simeq m_I$, exhibiting thawing behavior [41]. For our model to produce an effective crossing of the phantom divide from phantom (at large z) to quintessence (at small z), we need to activate first the dynamics of the NQ field. Therefore, we need $m_2 > m_1$. When this happens, ϕ_1 is still frozen, but ϕ_2 starts to roll down $V_2(\phi_2)$, i.e., it starts climbing up $\epsilon_2 V_2(\phi_2) = -V_2(\phi_2)$. Its energy density evolves to less negative values and its pressure to less positive values. As a consequence, the total energy density of the DE sector increases during this epoch. Finally, if $m_1 > H_0$, SQ starts to roll down $V_1(\phi_1)$ in the past – after the activation of NQ – and eventually, for appropriate initial conditions and masses, the energy density of NQ becomes derisory in front of that of SQ. From that moment until the present, the total DE behaves as quintessence. This transition occurs at redshift z_{cross} , defined by the condition $\dot{\phi}_2^2(z_{\text{cross}}) = \dot{\phi}_1^2(z_{\text{cross}})$. In the future, ϕ_1 will oscillate around the minimum of $V_1(\phi_1)$ and ϕ_2 around the maximum of $-V_2(\phi_2)$, leading to dilution laws of the form $\rho_I(a) \sim a^{-3}$ – negative in the case of NQ – and zero pressure.

In the matter-dominated epoch onward, the background dynamics are ruled by the following system of

differential equations formed by the Friedmann and the KG equations,

$$E^2(a) = \frac{\Omega_m^0 a^{-3} + \Omega_\Lambda^0 + \frac{1}{6} (M_1^2 \varphi_1^2 - M_2^2 \varphi_2^2)}{1 + \frac{a^2}{6} [(\varphi_1')^2 - (\varphi_2')^2]}, \quad (7)$$

$$\varphi_I'' + \varphi_I' \left[\frac{4}{a} - \frac{3\Omega_m^0 a^{-4}}{2E^2(a)} - \frac{a}{2} ((\varphi_1')^2 - (\varphi_2')^2) \right] + \frac{M_I^2 \varphi_I}{a^2 E^2(a)} = 0, \quad (8)$$

with $\Omega_m^0 = \rho_m^0/\rho_c^0$ and $\Omega_\Lambda^0 \equiv V_0/\rho_c^0$, and ρ_c^0 the current critical energy density in the universe. The primes denote derivatives with respect to the scale factor. For convenience, we use the following dimensionless quantities, $E \equiv H/H_0$, $M_I \equiv m_I/H_0$ and $\varphi_I \equiv (8\pi G)^{1/2} \phi_I$. The contribution of radiation can be added trivially. In practice, for the mass values of interest, the model reduces to Λ CDM during radiation domination, since $V_{\text{ini}} \ll \rho_r$ (cf. Eq. 6), and thus has no impact on the cosmic dynamics.

The model has four additional parameters compared to Λ CDM, namely, M_1 , M_2 , and the two initial field values, $\varphi_{1,\text{ini}}$ and $\varphi_{2,\text{ini}}$. It reduces to the standard model if $M_1, M_2 \ll H_0$ or if the initial scalar fields sit already on the minima of $V_{1,2}$. The initial values of the field derivatives, $\dot{\varphi}_{1,\text{ini}}$ and $\dot{\varphi}_{2,\text{ini}}$, are naturally set to zero, and Ω_Λ^0 is fixed through a shooting method to fulfill the consistency condition $E(a=1) = 1$.

Data and methodology – We employ state-of-the-art data from CMB, BAO and SNIa to constrain our model. In particular, we make use of compressed CMB information through the same correlated Gaussian prior on $(\theta_*, \omega_b, \omega_{bc})_{\text{CMB}}$ as in [10], which is based on *Planck*'s *CamSpec* CMB likelihood [42]. This is sufficient, since our model only introduces new physics in the late universe. We also use the BAO data from DESI Data Release 2 (DR2) [10] and the SNIa from DES-Y5 [43, 44]. We restrict our exploration of the parameter space to the region where φ_I exhibit no oscillations at present by using the prior $0 \leq M_1 < M_2 \leq 10$.

Our model is implemented in a modified version of **CLASS** [45, 46], which allows us to compute all the needed background observables. The exploration of the parameter space and the extraction of the Monte Carlo Markov chains is carried out with **Cobaya** [47], and the resulting chains are analyzed with **GetDist** [48].

Results – Our fitting results are displayed in Table I. We compare the performance of our model with those of Λ CDM and the Chevallier-Polarski-Linder (CPL) parametrization, in which DE is modeled as a perfect fluid with EoS $w(a) = w_0 + w_a(1-a)$ [50, 51]. We find that the CPL model yields a decrease in the minimum value of χ^2 , χ_{min}^2 , of ~ 19 units compared to Λ CDM, corresponding to a reduction in the Akaike Information Criterion (AIC) [52] of about 15 units. This suggests a very strong evidence for the CPL. The likelihood-ratio test [53, 54] also indicates a preference for the CPL model at 3.94σ CL, which is in perfect agreement with previous works, see, e.g., [10, 12, 55]. The χ_{min}^2 decreases at a

| Parameter | Λ CDM | CPL | SQ+NQ |
|--------------------------|-------------------|-------------------------|------------------------|
| Ω_m^0 | 0.302 ± 0.005 | 0.321 ± 0.007 | 0.315 ± 0.006 |
| H_0 | 68.35 ± 0.50 | 66.17 ± 0.86 | 67.06 ± 0.57 |
| M_1 | — | — | $2.4^{+0.4}_{-0.9}$ |
| M_2 | — | — | $6.5^{+1.8}_{-2.2}$ |
| $\varphi_{1,\text{ini}}$ | — | — | 0.67 ± 0.18 |
| $\varphi_{2,\text{ini}}$ | — | — | $0.34^{+0.06}_{-0.12}$ |
| w_0 | — | -0.752 ± 0.062 | — |
| w_a | — | $-0.90^{+0.27}_{-0.24}$ | — |
| χ_{min}^2 | 1666.33 | 1647.48 | 1648.04 |
| $E_{\Lambda\text{CDM}}$ | — | 3.94σ | 3.27σ |

TABLE I. Mean values and uncertainties at 68% CL obtained using Planck+DESI+DES-Y5 for the Λ CDM, CPL and SQ+NQ, from the corresponding one-dimensional posterior distributions. We also display the minimum values of χ^2 and the statistical exclusion level of Λ CDM, as in [10, 12].

similar level – by ~ 18 units compared to Λ CDM – when moving to the SQ+NQ model. Taking into account that the latter has 4 more parameters than the Λ CDM, the AIC in this case is ~ 10 units smaller than in the standard model. This translates into a preference of SQ+NQ over Λ CDM at 3.27σ CL.

We have checked that our model suffers from non-negligible volume effects. The one-dimensional profile likelihoods for M_1 and M_2 shown in the right plots of Fig. 2 – obtained following the method of Ref. [56] – demonstrate that there is a wide range of masses – namely, $2 \lesssim M_1 \lesssim 4$, $4 \lesssim M_2 \lesssim 9$ – that lead to low values of χ^2 . In any case, these marginalization effects do not bias our conclusions, as the latter are solely based on the χ_{min}^2 values of each model.

The left and central plots of Fig. 2 show that our model is perfectly able to produce shapes of $H(z)$ and the normalized DE energy density $f_{\text{DE}}(z) = \rho_{\text{DE}}(z)/\rho_{\text{DE}}^0$ in the 1σ region of the model-agnostic reconstructions obtained using CMB+BAO+SNIa [12]. Notice that neither of the two components forming the composite DE sector crosses the phantom divide, cf. the central upper plot. However, the effective EoS parameter, defined as $w_{\text{DE}}(z) = (p_1(z) + p_2(z))/(\rho_1(z) + \rho_2(z))$ does exhibit a transition from phantom – despite there is no phantom DE – to quintessence. Fig. 2 also demonstrates that thawing quintessence can fit the data better than Λ CDM but falls short in front of models with crossing, a conclusion reached also by other authors [57, 58].

We remark that our results are highly non-trivial. The phenomenology required to fit the data cannot be reproduced by two perfect fluids with constant EoS parameters plus a cosmological constant, even if one of the fluids is allowed to have negative energy density and positive pressure, as NQ. Let us show that explicitly. In such a scenario, the normalized DE density reads,

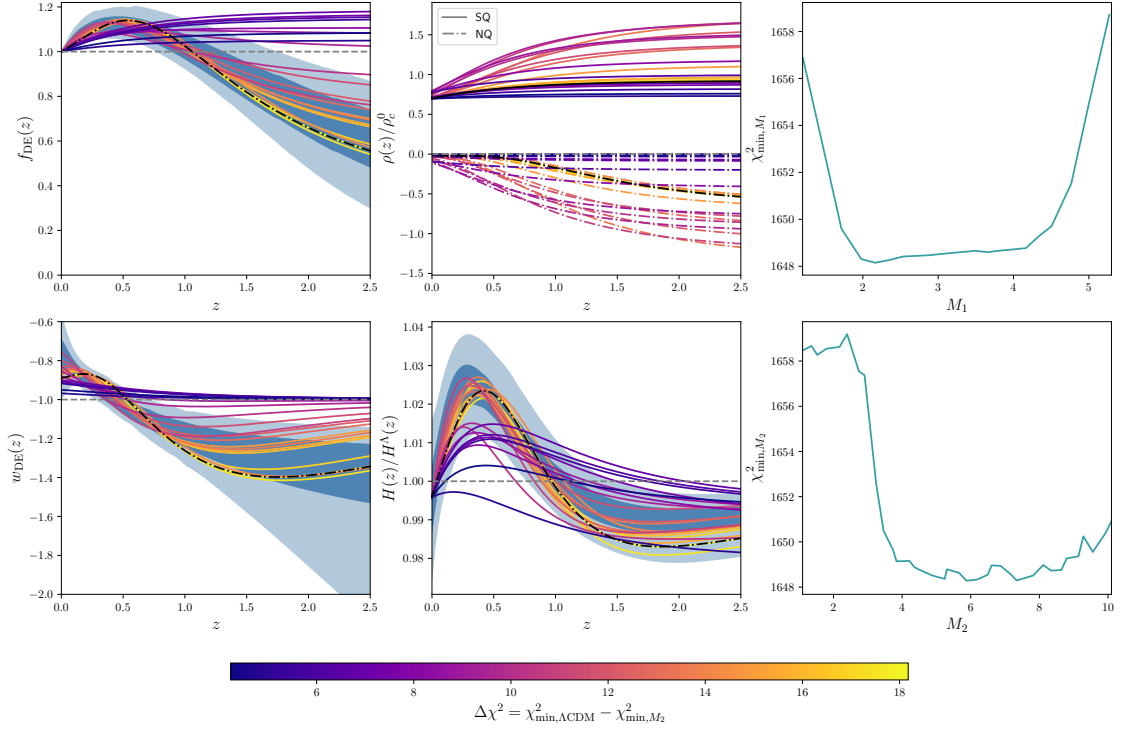


FIG. 2. *Right plots:* Profile distributions for M_1 and M_2 . A wide range of masses lead to low values of χ^2 ; *Left and central plots:* In addition to the reconstructions obtained with Planck+DESI+DES-Y5 [12] for the relevant background quantities (shown in light blue), we display several curves associated to SQ+NQ models with varying ability to describe the data. We use models corresponding to different points on the profile likelihood of M_2 , with the best-fit model shown as a black dot-dashed line. For the Λ CDM $H^\Lambda(z)$ we set $\Omega_m^0 = 0.315$ and $H_0 = 67.26$ km/s/Mpc [49]. In the central upper plot, we show the SQ and NQ densities that contribute to the total DE density in solid and dashed curves, respectively.

$$f_{\text{DE}}(z) = \frac{1 - \Omega_m^0 + \Omega_1^0[(1+z)^{\xi_1} - 1] + \Omega_2^0[(1+z)^{\xi_2} - 1]}{1 - \Omega_m^0}, \quad (9)$$

with $\xi_i \equiv 3(1+w_i)$ for $i = 1, 2$. We want this function to satisfy, at least, these three conditions: (i) $f(z = 0.4) \sim 1.1$; (ii) $df/dz = 0$ at $z \sim 0.4$; and $f(z \sim 1.1) = 0$. All of them are fulfilled in good approximation by our reconstruction [12], cf. Fig. 2. Using the conditions (i)+(ii) and (ii)+(iii) we obtain, respectively,

$$\Omega_1^0(\xi_1, \xi_2) = \frac{0.1(1 - \Omega_m^0)}{1.4\xi_1 - 1 - \frac{\xi_1}{\xi_2}1.4\xi_1 - \xi_2(1.4\xi_2 - 1)}. \quad (10)$$

$$\Omega_1^0(\xi_1, \xi_2) = \frac{\Omega_m^0 - 1}{2.1\xi_1 - 1 - \frac{\xi_1}{\xi_2}1.4\xi_1 - \xi_2(2.1\xi_2 - 1)}, \quad (11)$$

By equating these two expressions we could find in principle an equation that relates ξ_1 and ξ_2 . However, they describe two-dimensional surfaces that do not intersect

each other, so there is no point (ξ_1, ξ_2) that fulfills the required conditions. This is telling us that, besides the presence of NQ, the thawing behavior of the SQ field is important for the success of the SQ+NQ model. Note that the phenomenology of this model is equivalent to that of one with SQ potential $V_1 = m_1^2\phi_1^2/2$ and a phantom field with $V_2 = V_0 - m_2^2\phi_2^2/2$; or to a model with phantom DE and phantom matter, given suitable potentials – even though these species occupy completely different regions of the EoS diagram (cf. Fig. 1).

Conclusions – The persistent hints of dynamical dark energy offer a valuable opportunity in the quest to understand its fundamental nature. With this in mind, it is essential to distinguish which features are genuinely supported by the data, rather than being spurious artifacts of specific models or parametrizations. The CPL parametrization provides a great fit to the current CMB+BAO+SN Ia data, and it suggests a crossing of the phantom divide, which has caused much concern. On the other hand, it is well known that if DE consists of a single scalar field slowly rolling down its potential its EoS cannot cross $w = -1$, although a fit through the lens of CPL

could lead us to the opposite conclusion [59]. To more precisely assess the degree of evidence for a crossing of the phantom divide, we applied in [12] a model-agnostic reconstruction of the DE EoS and its energy density and quantified the probability of crossing to be of 96.21% to 99.97%, see also [14–16]. In view of these results, it is worthwhile to investigate whether the peak observed in f_{DE} at $z \sim 0.4 - 0.5$ can be realized within a model derived from an action-based formulation.

In this *Letter*, we show that this phenomenology can be produced without a true crossing of the phantom divide, considering only two minimally coupled scalar fields. The effective DE resulting from the combination of standard and negative quintessence can replicate the required shape of the background quantities of interest. NQ has negative energy density and positive pressure, both of which decrease in absolute value with the expansion. The two fields are characterized by their mass and initial field value (besides one positive cosmological constant). We compare the performance of this model with Λ CDM and the CPL parametrization. Our model outperforms Λ CDM – by ~ 18 units of χ^2_{min} – and describes the CMB+BAO+SN Ia data at a similar level to CPL. The standard model is excluded at 3.94σ for CPL and 3.27σ for SQ+NQ. The slight decrease of significance in our model is due to the introduction of two additional parameters. We have also shown that the preferred DE evolution cannot be reproduced by two perfect fluids

with constant EoS parameters plus a cosmological constant, most probably because the component mimicking SQ cannot exhibit in this case thawing behavior.

It will be important to further explore the implications of the SQ+NQ model. We have verified that the region of parameter space leading to scalar field oscillations at low z also yields very competitive results. We plan to study this region in more detail and provide a comprehensive analysis of volume effects in an extended paper.

Additionally, it would be interesting to compare our model with others that produce similar phenomenology [20, 21, 23, 24, 26, 27, 60], particularly at the perturbative level. For instance, modifications to the Poisson equation in non-minimally coupled scalar field scenarios could lead to distinctive signatures in the growth of large-scale structures, even when the background evolution is nearly identical. We also leave this investigation for future work.

Acknowledgments – The authors are funded by “la Caixa” Foundation (ID 100010434) and the European Union’s Horizon 2020 research and innovation programme under the Marie Skłodowska-Curie grant agreement No 847648, with fellowship code LCF/BQ/PI23/11970027. They acknowledge the participation in the COST Action CA21136 “Addressing observational tensions in cosmology with systematics and fundamental physics” (CosmoVerse), and thank Prof. Joan Solà and Prof. Jaume Garriga for helpful discussions.

-
- [1] V. Sahni, A. Shafieloo, and A. A. Starobinsky, Model independent evidence for dark energy evolution from Baryon Acoustic Oscillations, *Astrophys. J. Lett.* **793**, L40 (2014), arXiv:1406.2209 [astro-ph.CO].
 - [2] V. Salvatelli, N. Said, M. Bruni, A. Melchiorri, and D. Wands, Indications of a late-time interaction in the dark sector, *Phys. Rev. Lett.* **113**, 181301 (2014), arXiv:1406.7297 [astro-ph.CO].
 - [3] J. Solà, A. Gómez-Valent, and J. de Cruz Pérez, Hints of dynamical vacuum energy in the expanding Universe, *Astrophys. J. Lett.* **811**, L14 (2015), arXiv:1506.05793 [gr-qc].
 - [4] J. Solà, A. Gómez-Valent, and J. de Cruz Pérez, First evidence of running cosmic vacuum: challenging the concordance model, *Astrophys. J.* **836**, 43 (2017), arXiv:1602.02103 [astro-ph.CO].
 - [5] J. Solà Peracaula, J. de Cruz Pérez, and A. Gómez-Valent, Dynamical dark energy vs. $\Lambda = \text{const}$ in light of observations, *EPL* **121**, 39001 (2018), arXiv:1606.00450 [gr-qc].
 - [6] G.-B. Zhao *et al.*, Dynamical dark energy in light of the latest observations, *Nature Astron.* **1**, 627 (2017), arXiv:1701.08165 [astro-ph.CO].
 - [7] J. Solà Peracaula, J. de Cruz Pérez, and A. Gómez-Valent, Possible signals of vacuum dynamics in the Universe, *Mon. Not. Roy. Astron. Soc.* **478**, 4357 (2018), arXiv:1703.08218 [astro-ph.CO].
 - [8] J. Solà, A. Gómez-Valent, and J. de Cruz Pérez, The H_0 tension in light of vacuum dynamics in the Universe, *Phys. Lett. B* **774**, 317 (2017), arXiv:1705.06723 [astro-ph.CO].
 - [9] J. Solà Peracaula, A. Gómez-Valent, and J. de Cruz Pérez, Signs of Dynamical Dark Energy in Current Observations, *Phys. Dark Univ.* **25**, 100311 (2019), arXiv:1811.03505 [astro-ph.CO].
 - [10] M. Abdul Karim *et al.* (DESI), DESI DR2 Results II: Measurements of Baryon Acoustic Oscillations and Cosmological Constraints, (2025), arXiv:2503.14738 [astro-ph.CO].
 - [11] K. Lodha *et al.* (DESI), Extended Dark Energy analysis using DESI DR2 BAO measurements, (2025), arXiv:2503.14743 [astro-ph.CO].
 - [12] A. González-Fuentes and A. Gómez-Valent, Reconstruction of dark energy and late-time cosmic expansion using the Weighted Function Regression method, (2025), arXiv:2506.11758 [astro-ph.CO].
 - [13] J.-X. Li and S. Wang, Reconstructing dark energy with model independent methods after DESI DR2 BAO, (2025), arXiv:2506.22953 [astro-ph.CO].
 - [14] R. E. Keeley, A. Shafieloo, and W. L. Matthewson, Could We Be Fooled about Phantom Crossing?, (2025), arXiv:2506.15091 [astro-ph.CO].
 - [15] E. Özlüker, E. Di Valentino, and W. Giarè, Dark Energy Crosses the Line: Quantifying and Testing the Evidence for Phantom Crossing, (2025), arXiv:2506.19053 [astro-ph.CO].

- [16] E. Silva and R. C. Nunes, Testing Signatures of Phantom Crossing through Full-Shape Galaxy Clustering Analysis, (2025), arXiv:2507.13989 [astro-ph.CO].
- [17] W. Fang, W. Hu, and A. Lewis, Crossing the Phantom Divide with Parameterized Post-Friedmann Dark Energy, Phys. Rev. D **78**, 087303 (2008), arXiv:0808.3125 [astro-ph].
- [18] Y.-F. Cai, E. N. Saridakis, M. R. Setare, and J.-Q. Xia, Quintom Cosmology: Theoretical implications and observations, Phys. Rept. **493**, 1 (2010), arXiv:0909.2776 [hep-th].
- [19] Y. Cai, X. Ren, T. Qiu, M. Li, and X. Zhang, The Quintom theory of dark energy after DESI DR2, (2025), arXiv:2505.24732 [astro-ph.CO].
- [20] G. Ye, M. Martinelli, B. Hu, and A. Silvestri, Hints of Nonminimally Coupled Gravity in DESI 2024 Baryon Acoustic Oscillation Measurements, Phys. Rev. Lett. **134**, 181002 (2025), arXiv:2407.15832 [astro-ph.CO].
- [21] G. Ye, Bridge the Cosmological Tensions with Thawing Gravity, (2024), arXiv:2411.11743 [astro-ph.CO].
- [22] Y. Tiwari, U. Upadhyay, and R. K. Jain, Exploring cosmological imprints of phantom crossing with dynamical dark energy in Horndeski gravity, Phys. Rev. D **111**, 043530 (2025), arXiv:2412.00931 [astro-ph.CO].
- [23] W. J. Wolf, C. García-García, T. Anton, and P. G. Ferreira, Assessing cosmological evidence for non-minimal coupling, (2025), arXiv:2504.07679 [astro-ph.CO].
- [24] A. Chakraborty, P. K. Chanda, S. Das, and K. Dutta, DESI results: Hint towards coupled dark matter and dark energy, (2025), arXiv:2503.10806 [astro-ph.CO].
- [25] S. L. Guedezounme, B. R. Dinda, and R. Maartens, Phantom crossing or dark interaction?, (2025), arXiv:2507.18274 [astro-ph.CO].
- [26] S. D. Odintsov, D. Sáez-Chillón Gómez, and G. S. Sharov, Modified gravity/dynamical dark energy vs Λ CDM: is the game over?, Eur. Phys. J. C **85**, 298 (2025), arXiv:2412.09409 [gr-qc].
- [27] S. Nojiri, S. D. Odintsov, and V. K. Oikonomou, Phantom Crossing and Oscillating Dark Energy with $F(R)$ Gravity, (2025), arXiv:2506.21010 [gr-qc].
- [28] D. Camarena, K. Greene, J. Houghteling, and F.-Y. Cyr-Racine, DESigning concordant distances in the age of precision cosmology: the impact of density fluctuations, (2025), arXiv:2507.17969 [astro-ph.CO].
- [29] R. R. Caldwell, A Phantom menace?, Phys. Lett. B **545**, 23 (2002), arXiv:astro-ph/9908168.
- [30] B. Feng, X.-L. Wang, and X.-M. Zhang, Dark energy constraints from the cosmic age and supernova, Phys. Lett. B **607**, 35 (2005), arXiv:astro-ph/0404224.
- [31] D. E. Kaplan and R. Sundrum, A Symmetry for the cosmological constant, JHEP **07**, 042, arXiv:hep-th/0505265.
- [32] S. M. Carroll, M. Hoffman, and M. Trodden, Can the dark energy equation-of-state parameter w be less than -1 ?, Phys. Rev. D **68**, 023509 (2003), arXiv:astro-ph/0301273.
- [33] J. M. Cline, S. Jeon, and G. D. Moore, The Phantom menaced: Constraints on low-energy effective ghosts, Phys. Rev. D **70**, 043543 (2004), arXiv:hep-ph/0311312.
- [34] R. Emparan and J. Garriga, Non-perturbative materialization of ghosts, JHEP **03**, 028, arXiv:hep-th/0512274.
- [35] J. Garriga and A. Vilenkin, Living with ghosts in Lorentz invariant theories, JCAP **01**, 036, arXiv:1202.1239 [hep-th].
- [36] L. Amendola and S. Tsujikawa, *Dark Energy: Theory and Observations* (Cambridge University Press, 2015).
- [37] J. Grande, J. Solà Peracaula, and H. Stefancic, Λ XCDM: A Cosmon model solution to the cosmological coincidence problem?, JCAP **08**, 011, arXiv:gr-qc/0604057.
- [38] N. E. Mavromatos and J. Solà Peracaula, Inflationary physics and trans-Planckian conjecture in the stringy running vacuum model: from the phantom vacuum to the true vacuum, Eur. Phys. J. Plus **136**, 1152 (2021), arXiv:2105.02659 [hep-th].
- [39] A. Gómez-Valent and J. Solà Peracaula, Phantom Matter: A Challenging Solution to the Cosmological Tensions, Astrophys. J. **975**, 64 (2024), arXiv:2404.18845 [astro-ph.CO].
- [40] A. Gómez-Valent and J. Solà Peracaula, Composite dark energy and the cosmological tensions, Phys. Lett. B **864**, 139391 (2025), arXiv:2412.15124 [astro-ph.CO].
- [41] R. R. Caldwell and E. V. Linder, The Limits of quintessence, Phys. Rev. Lett. **95**, 141301 (2005), arXiv:astro-ph/0505494.
- [42] P. Lemos and A. Lewis, CMB constraints on the early Universe independent of late-time cosmology, Phys. Rev. D **107**, 103505 (2023), arXiv:2302.12911 [astro-ph.CO].
- [43] M. Vincenzi *et al.* (DES), The Dark Energy Survey Supernova Program: Cosmological Analysis and Systematic Uncertainties, Astrophys. J. **975**, 86 (2024), arXiv:2401.02945 [astro-ph.CO].
- [44] T. M. C. Abbott *et al.* (DES), The Dark Energy Survey: Cosmology Results with ~ 1500 New High-redshift Type Ia Supernovae Using the Full 5 yr Data Set, Astrophys. J. Lett. **973**, L14 (2024), arXiv:2401.02929 [astro-ph.CO].
- [45] J. Lesgourgues, The cosmic linear anisotropy solving system (class) i: Overview (2011), arXiv:1104.2932 [astro-ph.IM].
- [46] D. Blas, J. Lesgourgues, and T. Tram, The cosmic linear anisotropy solving system (class). part ii: Approximation schemes, Journal of Cosmology and Astroparticle Physics **2011** (07), 034–034.
- [47] J. Torrado and A. Lewis, Cobaya: Code for Bayesian Analysis of hierarchical physical models, JCAP **05**, 057, arXiv:2005.05290 [astro-ph.IM].
- [48] A. Lewis, GetDist: a Python package for analysing Monte Carlo samples, (2019), arXiv:1910.13970 [astro-ph.IM].
- [49] E. Rosenberg, S. Gratton, and G. Efsthathiou, CMB power spectra and cosmological parameters from Planck PR4 with CamSpec, Mon. Not. Roy. Astron. Soc. **517**, 4620 (2022), arXiv:2205.10869 [astro-ph.CO].
- [50] M. Chevallier and D. Polarski, Accelerating universes with scaling dark matter, Int. J. Mod. Phys. D **10**, 213 (2001), arXiv:gr-qc/0009008.
- [51] E. V. Linder, Exploring the expansion history of the universe, Phys. Rev. Lett. **90**, 091301 (2003), arXiv:astro-ph/0208512.
- [52] H. Akaike, A new look at the statistical model identification, IEEE Transactions on Automatic Control **19**, 716 (1974).
- [53] J. Neyman and E. Pearson, On the Problem of the Most Efficient Tests of Statistical Hypotheses, Phil. Trans. Roy. Soc. Lond. A **231**, 289 (1933).
- [54] S. S. Wilks, The large-sample distribution of the likelihood ratio for testing composite hypotheses, The Annals of Mathematical Statistics **9**, 60 (1938).
- [55] W. Giarè, T. Mahassen, E. Di Valentino, and S. Pan, An overview of what current data can (and cannot yet) say

- about evolving dark energy, *Phys. Dark Univ.* **48**, 101906 (2025), arXiv:2502.10264 [astro-ph.CO].
- [56] A. Gómez-Valent, Fast test to assess the impact of marginalization in Monte Carlo analyses and its application to cosmology, *Phys. Rev. D* **106**, 063506 (2022), arXiv:2203.16285 [astro-ph.CO].
 - [57] W. J. Wolf, C. García-García, D. J. Bartlett, and P. G. Ferreira, Scant evidence for thawing quintessence, *Phys. Rev. D* **110**, 083528 (2024), arXiv:2408.17318 [astro-ph.CO].
 - [58] I. D. Gialamas, G. Hütsi, M. Raidal, J. Urrutia, M. Vassar, and H. Veermäe, Quintessence and phantoms in light of DESI 2025, (2025), arXiv:2506.21542 [astro-ph.CO].
 - [59] W. J. Wolf and P. G. Ferreira, Underdetermination of dark energy, *Phys. Rev. D* **108**, 103519 (2023), arXiv:2310.07482 [astro-ph.CO].
 - [60] P. Brax, Weinberg’s theorem, phantom crossing and screening, (2025), arXiv:2507.16723 [astro-ph.CO].